INTERNATIONAL LARGE DETECTOR

I D R

ILD Detector Collaboration

2018

ILD Editors

Main Editors:
Ties Behnke, Kiyotomo Kawagoe

Detector layout, technologies and Integration:
Karsten Buesser, Claude Vallee

Physics:
Keisuke Fujii, Jenny List

Software:
Frank Gaede, Akiya Miyamoto

Performance:
Keisuke Fujii, Jenny List

Costing:
Henri Videau, Karsten Buesser

Contents

Chapter 1
Introduction

Ties Behnke, Kiyotomo Kawagoe
2 pages

The ILD detector is a proposed detector for the international linear collider, ILC. It has been developed over the last 10 years within a proto-collaboration with the goal to develop and eventually propose a fully integrated detector for the ILC.

The fundamental ideas and concepts behind the ILD detector have been discussed in two previous documents, the letter of intent [1] and the detailed baseline document, DBD [**?**]. This document summarises the overall design of the detector, describes developments since the publishing of the DBD, and describes in more detail an effort to optimize the ILD detector.

The ILD detector concept has been designed as a multi-purpose detector. It should deliver excellent physics performance for collision energies between 90 Gev and 1 TeV, the largest possible energy reach of the ILC. The ILD detector has been optimized to perform excellently at the initial ILC energy of 250 GeV.

The science which will be done at the ILC requires a true multi-purpose detector. A central element of the design has been the capability of the detector to reconstruct precisely complex hadronic final states as well as more events with leptons or missing energy in the final state. Thus traditional precision detector elements as vertex detectors are combined in an overall design philosophy called particle flow, which has been developed for optimal hadronic event reconstruction.

The high precision vertex detector positioned very closely to the interaction point is followed by a hybrid tracking layout, realised as a combination of silicon tracking with a time projection chamber, and a calorimeter system. The complete system is located inside a large solenoid providing a magnetic field of 3.5-4 T. On the outside of the coil, the iron return yoke is instrumented as a muon system and as a tail catcher calorimeter.

The vertex detector is realised as a multi-layer pixel-vertex detector (VTX), with three super-layers each comprising two layers. The detector has a pure barrel geometry. To minimise the occupancy from background hits, the first super-layer is only half as long as the outer two. Whilst the underlying detector technology has not yet been decided, the VTX is optimised for point resolution and minimum material thickness.

A system of silicon strip and pixel detectors surrounds the VTX detector. In the barrel, two layers of silicon strip detectors (SIT) are arranged to bridge the gap between the VTX and the TPC. In the forward region, a system of two silicon-pixel disks and five silicon-strip disks (FTD) provides low angle tracking coverage.

A distinct feature of ILD is a large volume time projection chamber (TPC) with up to 224 points per track. The TPC is optimised for 3-dimensional point resolution and minimum material in the field cage and in the end-plate. It also allows $\mathrm{d}E/\mathrm{d}x$ based particle identification.

Outside the TPC a system of Si-strip detectors in between the TPC and the ECAL (SET), provide additional high precision space points which improve the tracking performance and provide additional redundancy in the regions between the main tracking volume and the calorimeters.

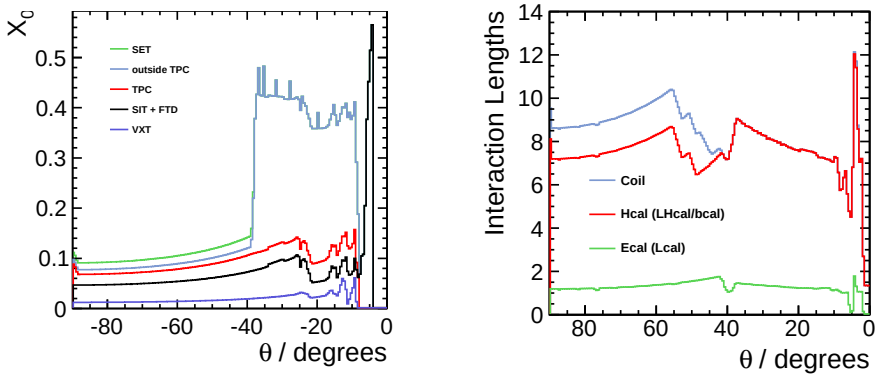

Figure I-1.1
Left: Average total radiation length of the material in the tracking detectors as a function of polar angle. Right: Total interaction length in the detector, up to the end of the calorimeter system, and including the coil of the detector.

A highly segmented electromagnetic calorimeter (ECAL) provides up to 30 samples in depth and small transverse cell size, split into a barrel and an end cap system. For the absorber Tungsten has been chosen, for the sensitive area silicon diodes or scintillator strips are considered.

This is followed by a segmented hadronic calorimeter (HCAL) with up to 48 longitudinal samples and small transverse cell size. Two options are considered, both based on a Steel-absorber structure. One option uses scintillator tiles of $3 \times 3\,\mathrm{cm}^2$, which are read out with an analogue system. The second uses a gas-based readout which allows a $1 \times 1\,\mathrm{cm}^2$ cell geometry with a semi-digital readout of each cell.

At very forward angles, below the coverage provided by the ECAL and the HCAL, a system of high precision and radiation hard calorimetric detectors (LumiCAL, BeamCAL, LHCAL) is foreseen. These extend the calorimetric coverage to almost 4π, measure the luminosity, and monitor the quality of the colliding beams.

A large volume superconducting coil surrounds the calorimeters, creating an axial B-field of nominally 3.5-4 Tesla.

An iron yoke, instrumented with scintillator strips or resistive plate chambers (RPCs), returns the magnetic flux of the solenoid, and, at the same time, serves as a muon filter, muon detector and tail catcher calorimeter.

The main parameters of the ILD detector are summarised in Table I-1.1 and table I-1.2.

The performance of the ILD concept has been extensively studied using a detailed GEANT4 based simulation model and sophisticated reconstruction tools. Backgrounds have been taken into account to the best of current knowledge. A key characteristics of the detector is the amount of material in the detector. Particle flow requires a thin tracker, to minimise interactions before the calorimeters, and thick calorimeters, to fully absorb the showers. Figure **??** (left) shows the material in the detector in radiation lengths, until the entry of the calorimeter. The right plot shows the total

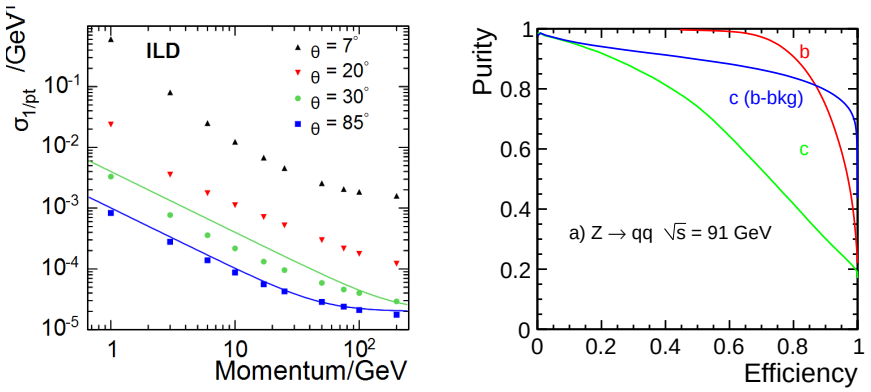

Figure I-1.2
(left) Momentum resolution for the ILD detector concept, as a function of the transverse momentum of the particle. (right) Flavour tagging efficiency versus purity for bottom events in sample of Z decays at 91 GeV, and for charm events with only bottom background.)

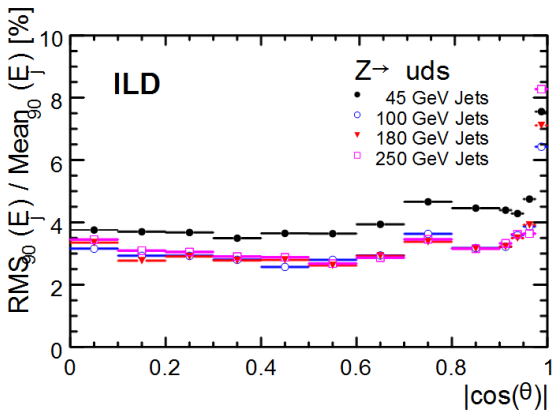

Figure I-1.3. Fractional jet energy resolution plotted against $|\cos\theta|$ where theta is the polar angle of the thrust axis of the event.

Table I-1.1. List of the main parameters of the ILD detector for the barrel part.

Barrel system						
System	R(in)	R(out) [mm]	z	comments		
VTX	16	60	125	3 double layers	Silicon pixel sensors,	
				layer 1:	layer 2:	layer 3-6
				$\sigma < 3\mu m$	$\sigma < 6\mu m$	$\sigma < 4\mu m$
Silicon						
- SIT	153	300	644	2 silicon strip layers	$\sigma = 7\mu m$	
- SET	1811		2300	2 silicon strip layers	$\sigma = 7\mu m$	
- TPC	330	1808	2350	MPGD readout	1×6mm^2 pads	$\sigma = 60\mu m$ at zero drift
ECAL	1843	2028	2350	W absorber	SiECAL	30 Silicon sensor layers, 5×5 mm^2 cells
					ScECAL	30 Scintillator layers, 5×45 mm^2 strips
HCAL	2058	3410	2350	Fe absorber	AHCAL	48 Scintillator layers, 3×3cm^2 cells, analogue
					SDHCAL	48 Gas RPC layers, 1×1 cm^2 cells, semi-digital
Coil	3440	4400	3950	3.5 T field	2λ	
Muon	4450	7755	2800	14 scintillator layers		

interaction length including the calorimeter system.

The performance of the tracking system can be summarised by its combined momentum resolution, shown in Figure I-8.7 (left). A resolution of $\sigma_{1/p_T} = 2 \times 10^{-5}\,\text{GeV}^{-1}$ has been achieved for high momenta. For many physics studies the tagging of long lived particles is of key importance. Several layers of pixel detectors close to the IP allow the reconstruction of displaced vertices, as shown in

Table I-1.2. List of the main parameters of the ILD detector for the end cap part.

End cap system						
System	z(min)	z(max) [mm]	r(min), r(max)	comments		
FTD	220	371		2 pixel disks	$\sigma = 2 - 6\mu m$	
				5 strip disks	$\sigma = 7\mu m$	
ETD	2420	2445	419-1822	2 silicon strip layers	$\sigma = 7\mu m$	
ECAL	2450	2635		W-absorber	SiECAL	Si readout layers
					ScECAL	Scintillator layers
HCAL	2650	3937	335-3190	Fe absorber	AHCAL	48 Scintillator layers 3×3cm^2 cells, analogue
					SDHCAL	48 gas RPC layers 1×1cm^2 cells, semi-digital
BeamCal	3595	3715	20-150	W absorber	30 GaAs readout layers	
Lumical	2500	2634	76-280	W absorber	30 Silicon layers	
LHCAL	2680	3205	93-331	W absorber		
Muon	2560		300-7755	12 scintillator layers		

Figure I-8.7 (right).

Calorimeter system and tracking system together enter into the particle flow performance. The performance of the ILD detector for different energies and as a function of the polar angle is shown in Figure I-1.3.

The few plots shown in this introduction illustrate the anticipated performance of the detector and illustrate the potential for precision measurements with the ILD detector. More details on the performance may be found in section **??** of this document.

In this document the current state of the design of the ILD detector is summarised. The technologies which are proposed for the different parts of the detector are introduced. An extensive benchmarking has been performed, to demonstrate the performance of the ILD detector. This has been done for two different detector implementations, a large and a smaller one. Both concepts are the result of intense optimization efforts, with different goals - cost effectivnes was foremost a criterium for the smaller one, ultimate performance for the larger model.

The ILD group who is proposing this detector has currently some 70 member institutes from all around the world. The group has evolved into a proto-collaboration, which is positioning itself to move forward with a proposal for a detector at the ILC at the moment that ILC becomes a real project.

A lot of the work presented in this report is based on intense R&D work which has taken place over the last decade to develop the necessary technologies. This work has typically happened within dedicated R&D collaborations, which are independent but maintain very close connections to ILD. All technologies selected by ILD for one of its subsystems have been proven experimentally to meet the performance goals, or to come very close.

Developing a very powerful detector concept over a long period of time requires balancing cutting edge technologies, which might become available while the concept is being developed, with safe and

sound solutions. ILD in many cases is pursuing more than one technological option, to remain flexible and to be able to adopt to new developments. The concept group wants to remain open and flexible to be prepared to select the most modern and most powerful technology once it is necessary. However a distinction is made between options and alternatives: while options have undergone an extensive R&D program and have passed critical proof-of-concept tests, alternatives are potentially interesting and promising technologies which have not matured to a similar level at the time of writing this document.

The document starts with a short review of the science goals of the ILC, and how the goals can be achieved today with the detector technologies at hand. After a discussion of the ILC and the environment in which the experiment will take place the detector is described in more detail. The integration of the different sub-systems into an integrated detector is discussed, as is the interface between the detector and the collider. This is followed by a concise summary of the benchmarking which has been performed in order to find an optimal balance between performance and cost. To this end the costing methodology used by ILD is presented, and a cost estimate for the detector in 2018 costs is presented. The report closes with a summary of the proposed detector and its performance.

Chapter 2
Science with ILC

Keisuke Fujii, Jenny List
2 pages

Executive summary of the scientific goals of the ILC. Emphasis on 250 GeV. Prepare connection to choice of physics benchmarks, where details will of course come in the actual performance section.

Chapter 3
The ILC Environment

Karsten Buesser, Keisuke Fujii
3 pages

Overall ILC constraints (could be adapted from LoI introduction)

Updated beam conditions since DBD: new L*, backgrounds, energy profile (main plots from machine study group).

Initial focus on 250 GeV with future upgrades to higher energies

Critical channels/issues at 250 GeV

Chapter 4
The ILD detector concept

Ties Behnke, Kiyotomo Kawagoe
pages

4.1 The overall ILD concept

The ILD overall concept: low tracker material, high granularity, particle flow, triggerless
Reminder of main arguments from the LoI reference for sizes, B, depth, etc
Detector performance aspects to be anticipated for higher energies

4.2 Optimising ILD

Chapter 5
Detector Layout and Technologies

Claude Vallee, Karsten Buesser
1 pages

5.1 Overall structure of the detector

Claude Vallee, Karsten Buesser
1 pages

5.1.1 Global structure and parameters

Reminder of the global structure of the ILD detector, focusing details on the main changes since DBD, and mentioning remaining open options like anti-DID.

Subdetector technical conveners
4 pages

5.1.2 Subdetecor layouts

Description of the latest baseline design of subdetectors, including open options. Each technology option description should indicate its advantages (pro) and critical aspects (cons) in respect to ILD specifications. Potential new capabilities for the future (e.g. calorimeter timing) should also be indicated.

Vertex detector (Besson, Ishikawa, Vos): nb layers, dimensions, technology options.

Internal silicon trackers (Besson, Vos, Vila): FTD disks, dimensions, technology per disk, SiT including pixel option, short discussion status outer TPC silicon layers

TPC (Colas, Sugiyama): structure and readout options (GEM, Micromegas)

ECAL (Brient, Ootani): mechanical layout and readout options (Si, Sc)

HCAL (Laktineh, Sefkow): mechanical options (Videau,TESLA and readout options (Sc, RPC)

VFS (Benhammou, Schuwalow): layout adapted to new L*, LUMICAL, BEAMCAL,LHCAL sensors

Iron instrumentation (Saveliev): sensitive layers in yoke baseline design and sensor structure

Subdetector conveners
pages

5.2 Subdetector technology status

This section is one of the main technical added values of the IDR. It should summarize all technological progress since the DBD, including beam tests of technological prototypes and ongoing spinoffs. It should also indicate the remaining steps to fulfil the ILD requirements, with a focus of critical aspects associated to each technology choice. For conciseness only the highlights should be illustrated, with all details to be referenced in technical publications. As regards illustrations it is proposed to stick to o(1-2) photo and o(1-2) plot for each technology.

Auguste Besson, Akimasa Ishikawa, Marcel Vos
3 pages

5.2.1 Vertex detector

CMOS spin-offs: ALPIDE (ALICE upgrade) and MIMOSIS (CBM), New PSIRA chip for ILD

DEPFET spin-off: BELLE-2, BEAST and first physics events

FPCCD long prototype and irradiation tests

Short mention of other options: SOI, etc

Low material support developments (PLUME ladder) and cooling studies

Marcel Vos, Ivan Vila
1 pages

5.2.2 Silicon inner tracking detectors

Above DEPFET developments and FTD thermo-mechanical mockup

Paul Colas, Akira Sugiyama
3 pages

5.2.3 Time projection chamber

TPC prototype for generic beam tests of all readout options, the gating scheme and cooling. Mention LYCORIS silicon telescope and new field cage in construction.

CO2 Cooling measurements

Successful gating achieved with GEM

GEM and Micromegas spacial and ionization resolutions

Ongoing technological developments: improved module planarity, GRIDPIX RO options, etc.

Jean Claude Brient, Wataru Ootani, Felix Sefkow, Imad Laktineh
5 pages

5.2.4 Calorimeters

Si-ECAL: technological prototype (incl long slab) beamtest results, CMS HGCAL spinoff.

Sc-ECAL results from new detector unit in construction.

AHCAL beamtest results from large technological prototype, CMS HGCAL spinoff.

SDHCAL beamtest results of large technological prototype at CERN, ongoing development of large chambers.

Yan Benhammou, Sergej Schuwalow
2 pages

5.2.5 Very forward detectors

LUMICAL sensors: Beam test of thinner prototypes with improved transverse resolution of e-showers

BEAMCAL and LHCAL developments

Valery Saveliev
1 pages

5.2.6 Iron instrumentation

Fermilab Scintillator detectors prototypes and performance tests

Chapter 6
ILD Global Integration

Karsten Buesser, Claude Vallee

pages

Karsten Buesser, Roman Poeschl, Toshiaki Tauchi
3 pages

6.1 Internal ILD integration

Subdetector interfaces and integration scheme including services. Short reminder of the overall ILD integration scheme (unchanged). Technical drawings (ideally from CAD files) showing interfaces (pipes, cables, supports) for each subdetector within ILD. New input is expected from the recently setup dedicated working group chaired by Roman to update the service paths based on subdetector Interface and Control Documents.

Among points to illustrate: Inner tracker services, TPC services, ECAL electrical interfaces, HCAL interfaces in TESLA option and Videau option, VFS cables, global scheme for cable paths.

Yasuhiro Sugimoto
1 pages

6.2 External ILD integration

Generic layout of the cavern, mentioning the current options for its configuration (TDR, Tohoku, YS).

Yasuhiro Sugimoto
1 pages

6.2.1 Cavern ancillary services

Summary of ancillary services from subdetectors in the cavern and on surface, as it will result from subdetector information to be provided in Yasuhiro's excel file.

ILD overall wish for utility space on the platform, the service gallery and the service cavern.

Matthew Wing, Taikan Suehara
2 pages

6.2.2 Data acquisition

Expected principles and sketch of the DAQ.

Summary of characteristics of subdetector data including data throughput and local filtering, based on DAQ information recently requested to all subdetectors.

EUDAQ developments towards combined DAQ systems for beamtests

Felix Sefkow, Henri Videau, Karsten Buesser, Roman Poeschl, Toshiaki Tauchi
3 pages

6.3 Mechanical structure and studies

Static deformations of both structure options (TESLA/Videau) including LLR-DESY crosscheck.

Dynamic behaviour of both structure options under reference earthquake spectra, including LLR-DESY crosscheck.

New insights on the above issues are expected from the dedicated group steered by Henri, Felix, Roman and Karsten. Crosschecks between DESY and LLR will most likely restrict to the barrel. A discussion of the endcap structure may also be included.

If available, results on the mechanical behaviour of other subdetectors (e.g. TPC) are also welcome.

Karsten Buesser, Uwe Schneekloth
3 pages

6.4 Coil and yoke studies

Baseline yoke design and discussion of possible lighter options including separation wall option.

Updated field maps for the baseline yoke design. Table of field maps at various locations (including stray fields) for various yoke options.

Progress on technological design of anti-DID (KEK/Toshiba/Hitachi) and corresponding field map.

Daniel Jeans, Yan Benhammou, Sergej Schuwalow
2 pages

6.5 Beam background studies

Beam-beam BG occupancies with/without anti-DID. New results are expected from Daniel soon to clarify the open points of previous studies and consolidate the estimations. The rates shown in the IDR should if possible be computed for the latest ILC250 beam conditions (input files available from Anne Schuetz).

It would also be good to provide hit maps from backscattered neutrons from the beamdump and from halo muons, possibly using input particle files from Anne Schuetz.

Graham Wilson
1 pages

6.6 Alignment/ calibration procedures

There was little progress here since the LOI/DBD. Most of the corresponding text of these documents could be recovered and summarized for the IDR, taking into account the latest considerations about in-situ calibration with particles/collisions and subdetector requirements.

Chapter 7
Physics and Detector Modelling

F.Gaede, A.Miyamoto
4 pages

Chapter 8
Detector and Physics Performance

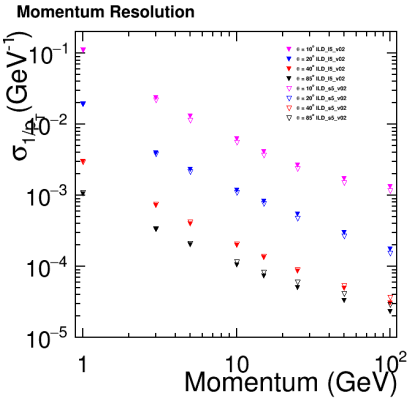

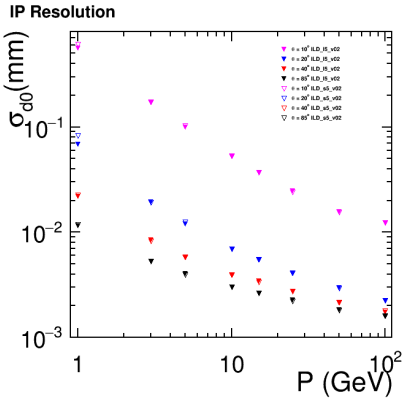

Figure I-8.1
Momentum (left) and impact parameter (right) resolution for the two ILD detector models, as a function of momentum of the single muon. Large detector: closed symbols - small detector: open symbols.

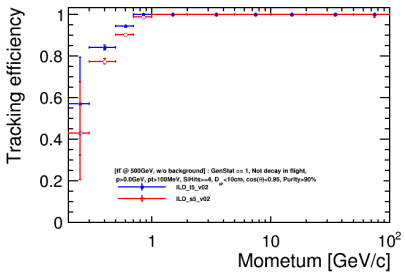

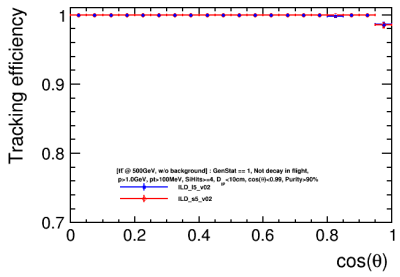

Figure I-8.2
Track finding efficiency for $t\bar{t}$-events at 500 GeV, as a function of momentum (left) and $cos(\theta)$ (right) for the large (red) and small (blue) ILD detector models.

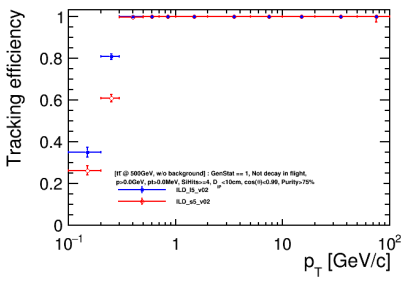

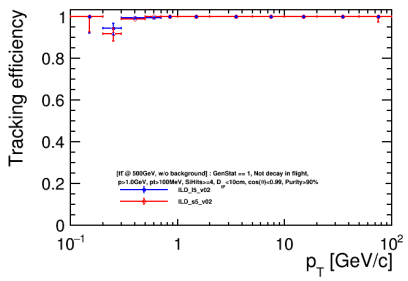

Figure I-8.3
Track finding efficiency for $t\bar{t}$-events at 500 GeV, as a function of transeverse momentum for the large (red) and small (blue) ILD detector models. left: $p > 0GeV$; right: $p > 1GeV$

Frank Gaede
5 pages

8.1 System performance

8.1.1 Vertexing

8.1.2 Tracking

Tracking Efficiency plots need to be redone with pair-bg overlaid !

8.1.3 Particle Flow performance and JER

8.1.4 Photon Reconstruction

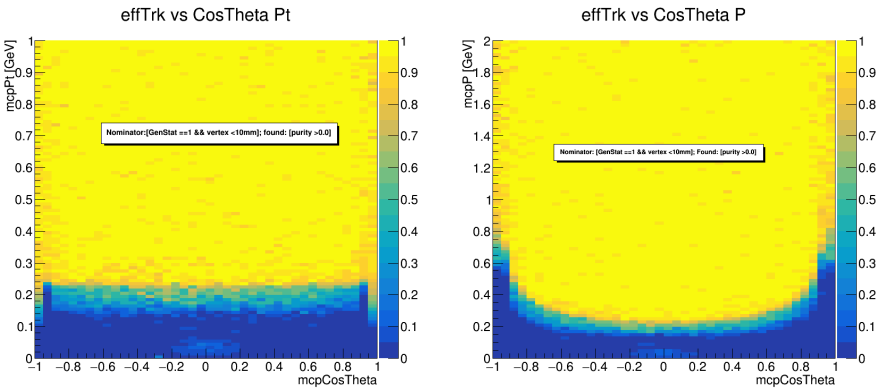

Figure I-8.4
Track finding efficiency for $t\bar{t}$-events at 500 GeV, as a function of transverse momentum (left), momentum (right) and $cos(\theta)$ for the large ILD detector model.

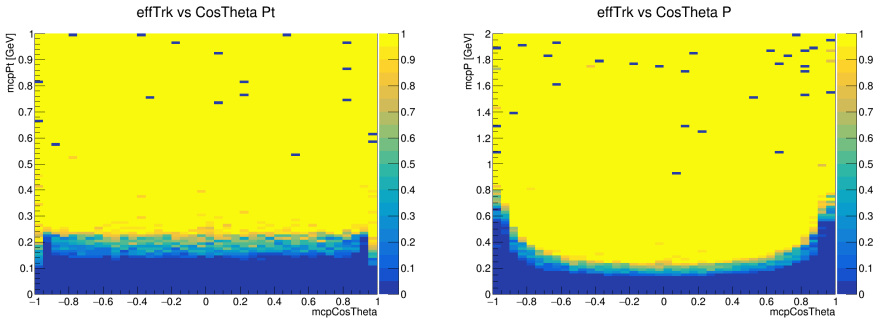

Figure I-8.5
Track finding efficiency for single muons as a function of transverse momentum (left), momentum (right) and $cos(\theta)$ for the large ILD detector model. FG: do we need these single particle eff. plots ?

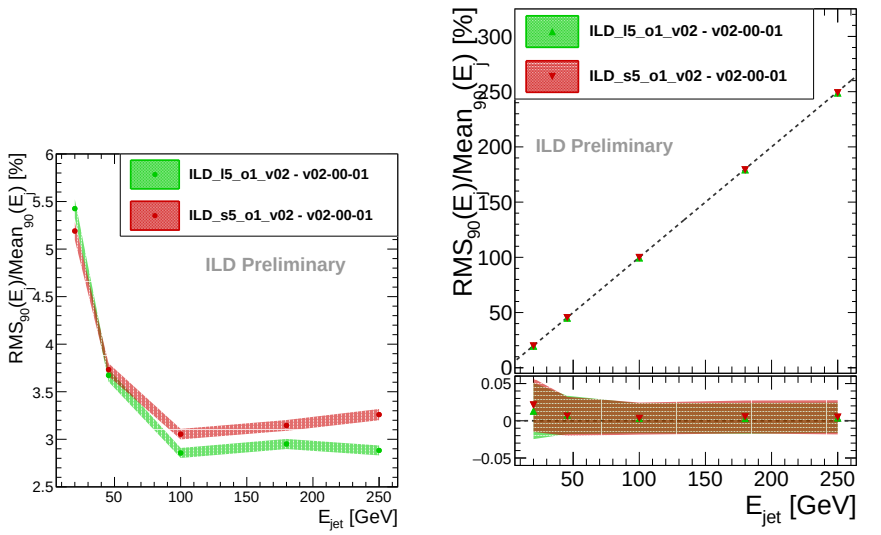

Figure I-8.6
Jet energy resolution (left) and jet energy scale (right) for the large and small ILD detector models as a function of the jet energy for uds di-jet events.

8.1.5 Lepton ID

muons, electrons

8.1.6 Charged Particle identification

Graham Wilson, Frank Gaede, Jenny List
5 pages

dE/dx, potentially ToF, shower shapes

8.2 High-level Reconstruction Performance

8.2.1 neutral

8.2.2 hadronically decaying tau ID

8.2.3 V0 / in flight decays vs radius

8.2.4 Baryons / Meson recosntruction

- $\Lambda_c^+ \to pK^-\pi^+$
- D^0, D^*
- $J\Psi \to \mu\mu$ / inclusive di-muon spectrum ?

8.2.5 Di-jet mass resolution between Cambridge and full physics

Keisuke Fujii, Jenny List
10 pages

- Z mass in $ZZ \to \nu\nu qq$, flavour separated
- W hadronic mass from $WW \to qql\nu$
- from Jakob $\nu\nu qqqq$
- various levels of cheating with TrueJet

8.3 Physics Benchmarks

8.3.1 General Remarks

8.3.2 Hadronic Branching Ratios of the Higgs Boson

8.3.3 Higgs Mass from $H \to b\bar{b}$

8.3.4 Branching Ratio of $H \to \mu^+\mu^-$

8.3.5 Sensitivity to $H \to$ invisible

8.3.6 τ decay modes and polarisation, A_{FB} and A_{LR} in $e^+e^- \to \tau^+\tau^-$

8.3.7 W mass, Triple Gauge Couplings and Beam Polarisation from $e^+e^- \to WW \to qql\nu$

8.3.8 Quartic Gauge Couplings in $e^+e^- \to \nu\nu qqqq$

8.3.9 A_{LR} and Jet Energy Scale Calibration from $e^+e^- \to \gamma Z$

8.3.10 A_{FB} and A_{LR} from $tt \to bbqqqq$

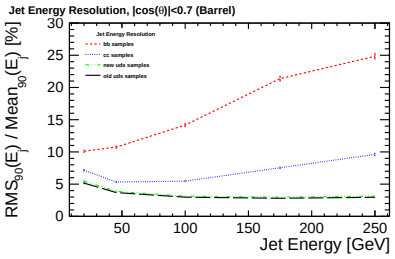

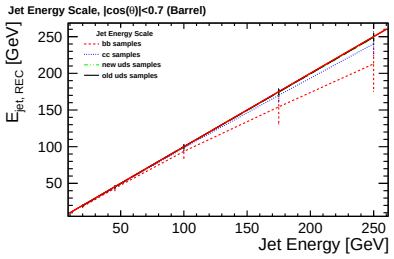

Figure I-8.7 Jet energy resolution (left) and jet energy scale (right) for cc and bb as a function of the jet energy compared to uds events.

Chapter 9
Costing

Chapter 10
Summary

Summary of the paper. Just a placeholder. Mastertest.

At this place, I try to annoy Thomas, for testing purposes — he is editing the same file at the same time in Overleaf, and we try to find out how well the merging / conflict handling tools really are.

Bibliography

[1] **ILD Concept Group**, T. Abe *et al.*, "The International Large Detector: Letter of Intent" arXiv:1006.3396 [hep-ex]. FERMILAB-LOI-2010-03, FERMILAB-PUB-09-682-E, DESY-2009-87, KEK-REPORT-2009-6.